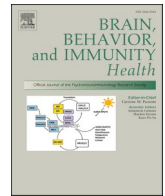


Contents lists available at [ScienceDirect](https://www.sciencedirect.com)

## Brain, Behavior, &amp; Immunity - Health

journal homepage: [www.editorialmanager.com/bbih/default.aspx](http://www.editorialmanager.com/bbih/default.aspx)

## Synapsin autoantibodies during pregnancy are associated with fetal abnormalities

Isabel Bünger<sup>a,b</sup>, Ivan Talucci<sup>c</sup>, Jakob Kreye<sup>a,b,d,e,f</sup>, Markus Höltje<sup>g</sup>,  
Konstantin L. Makridis<sup>e,f,h</sup>, Helle Foverskov Rasmussen<sup>a,b</sup>, Scott van Hoof<sup>f,a,b</sup>,  
César Cordero-Gomez<sup>a,b</sup>, Tim Ullrich<sup>e,f</sup>, Eva Sedlin<sup>e,f,i</sup>, Kai Oliver Kreissner<sup>c</sup>,  
Christian Hoffmann<sup>a</sup>, Dragomir Milovanovic<sup>a</sup>, Paul Turko<sup>g</sup>, Friedemann Paul<sup>j,k</sup>,  
Jessica Meckies<sup>l</sup>, Stefan Verlohren<sup>m</sup>, Wolfgang Henrich<sup>m</sup>, Rabih Chaoui<sup>n</sup>,  
Hans Michael Maric<sup>c</sup>, Angela M. Kaindl<sup>e,f,h</sup>, Harald Prüss<sup>a,b,\*</sup>

<sup>a</sup> German Center for Neurodegenerative Diseases (DZNE) Berlin, 10117, Berlin, Germany

<sup>b</sup> Department of Neurology and Experimental Neurology, Charité-Universitätsmedizin Berlin, Corporate Member of Freie Universität Berlin, Humboldt-Universität Berlin, and Berlin Institute of Health, 10117, Berlin, Germany

<sup>c</sup> Rudolf Virchow Center, Center for Integrative and Translational Bioimaging, University of Würzburg, Josef-Schneider-Str. 2, 97080, Würzburg, Germany

<sup>d</sup> Berlin Institute of Health (BIH), 10178, Berlin, Germany

<sup>e</sup> Department of Pediatric Neurology, Charité-Universitätsmedizin Berlin, Corporate Member of Freie Universität Berlin, Humboldt-Universität Berlin, and Berlin Institute of Health, 10117, Berlin, Germany

<sup>f</sup> Center for Chronically Sick Children, Charité- Universitätsmedizin Berlin, Corporate Member of Freie Universität Berlin, Humboldt-Universität Berlin, and Berlin Institute of Health, 10117, Berlin, Germany

<sup>g</sup> Institute of Integrative Neuroanatomy, Charité - Universitätsmedizin Berlin, Corporate Member of Freie Universität Berlin, Humboldt-Universität Berlin, and Berlin Institute of Health, 10117, Berlin, Germany

<sup>h</sup> Institute of Cell Biology and Neurobiology, Charité- Universitätsmedizin Berlin, Corporate Member of Freie Universität Berlin, Humboldt-Universität Berlin, and Berlin Institute of Health, 10117, Berlin, Germany

<sup>i</sup> Department of Neonatology, Helios Klinikum, Berlin-Buch, Germany

<sup>j</sup> NeuroCure Clinical Research Center, Charité - Universitätsmedizin Berlin, Corporate Member of Freie Universität Berlin, Humboldt-Universität Berlin, and Berlin Institute of Health, 10117, Berlin, Germany

<sup>k</sup> Experimental and Clinical Research Center, Max Delbrück Center for Molecular Medicine and Charité - Universitätsmedizin Berlin, 10117, Berlin, Germany

<sup>l</sup> Gynecology Practice Frauenärztinnen am Schloß, 12163, Berlin, Germany

<sup>m</sup> Department of Obstetrics, Charité – Universitätsmedizin Berlin, Corporate Member of Freie Universität Berlin, Humboldt-Universität Berlin, and Berlin Institute of Health, 10117, Berlin, Germany

<sup>n</sup> Center for Prenatal Diagnosis and Human Genetics, 10719, Berlin, Germany

## ARTICLE INFO

## Keywords:

Synapsin-I  
Antineuronal autoantibodies  
Transplacental transfer  
Maternofetal autoimmunity  
Growth retardation  
Peptide microarray

## ABSTRACT

Anti-neuronal autoantibodies can be transplacentally transferred during pregnancy and may cause detrimental effects on fetal development. It is unclear whether autoantibodies against synapsin-I, one of the most abundant synaptic proteins, are associated with developmental abnormalities in humans. We recruited a cohort of 263 pregnant women and detected serum synapsin-I IgG autoantibodies in 13.3% using cell-based assays. Seropositivity was strongly associated with abnormalities of fetal development including structural defects, intrauterine growth retardation, amniotic fluid disorders and neuropsychiatric developmental diseases in previous children (odds ratios of 3–6.5). Autoantibodies reached the fetal circulation and were mainly of IgG1/IgG3 subclasses. They bound to conformational and linear synapsin-I epitopes, five distinct epitopes were identified using peptide microarrays. The findings indicate that synapsin-I autoantibodies may be clinically useful biomarkers or even directly participate in the disease process of neurodevelopmental disorders, thus being potentially amenable to antibody-targeting interventional strategies in the future.

\* **Corresponding author.** German Center for Neurodegenerative Diseases (DZNE) Berlin, 10117, Berlin, Germany.

E-mail address: [harald.pruess@charite.de](mailto:harald.pruess@charite.de) (H. Prüss).

<https://doi.org/10.1016/j.bbih.2023.100678>

Received 19 August 2023; Accepted 21 August 2023

Available online 29 August 2023

2666-3546/© 2023 The Authors. Published by Elsevier Inc. This is an open access article under the CC BY-NC-ND license (<http://creativecommons.org/licenses/by-nc-nd/4.0/>).

## Abbreviations

CASPR2	contactin-associated protein-like 2
CBA	cell-based assay
ELISA	Enzyme-linked immunosorbent assay
HEK	Human embryonic kidney
NMDA	N-methyl-D-aspartate
SYN	synapsin
TKO	triple knockout mice
LLPS	liquid-liquid phase separation
SVs	synaptic vesicles

## 1. Introduction

Synapsins are neuron-specific phosphoproteins essential for neurotransmitter release and synaptic plasticity (De Camilli et al., 1990) by controlling the accessibility of synaptic vesicles for exocytosis via interactions with presynaptic proteins and the actin cytoskeleton (Zhang and Augustine, 2021). In mammals, three synapsin (SYN) genes *SYN1*, *SYN2*, and *SYN3* have been identified (Südhof et al., 1989). They encode ten isoforms with differentially regulated expression during neurodevelopment that coordinate neurite outgrowth and synapse formation (Fornasiero et al., 2010). Moreover, *SYN1* or *SYN2*, but not *SYN3* mutant mice displayed a severe epileptic phenotype with generalized seizures that manifested around two to three months of age (Rosahl et al., 1995). In line with these models, variants in *SYN1* were linked to an X-linked human phenotype comprising epilepsy, learning difficulties, macrocephaly, and aggressive behavior (MIM#300491, MIM#300115) (Garcia et al., 2004). Intriguingly, autoantibodies to synapsin-Ia/Ib have previously been identified in patients with limbic encephalitis and with various psychiatric and neurological disorders (Höltje et al., 2017). Despite the location of synapsin-I at the cytoplasmic site of synaptic vesicles, these patient-derived autoantibodies can reach their target via FcγII/III-mediated endocytosis and promote a reduction of synaptic vesicle density, thereby mimicking the human *SYN1* loss-of-function phenotype (Rocchi et al., 2019). While autoantibodies to synapsin and many further neuronal targets are increasingly detected in neurological disorders (Prüss, 2021), there is also growing evidence that antineuronal autoantibodies can act not only in affected individuals, but also in a fetus or neonate when diaplacentally transferred from their mother. In the gestational phase, the active placental transport of IgG antibodies, together with the yet premature fetal blood-brain barrier, may further augment the autoantibody exposure of the developing brain and thereby possibly result in long-lasting neuropsychiatric morbidity (Braniste et al., 2014). Such detrimental effects of diaplacentally transferred antineuronal autoantibodies have previously been shown in experimental transfer models of human autoantibodies against N-methyl-D-aspartate (NMDA) receptors (Jurek et al., 2019), contactin-associated protein 2 (CASPR2) (Brimberg et al., 2016), aquaporin 4 (Mader et al., 2022)<sup>13</sup>, and acetylcholine receptors (Coutinho et al., 2021).

We have recently reported an association of maternal synapsin-I autoantibodies with neurodevelopmental delay and epilepsy in the offspring (Bünger et al., 2023). However, the antibodies' prevalence in healthy pregnant women as well as the underlying target epitopes and association with neonatal/fetal outcomes are unknown. Thus, we here exploratively investigated synapsin-I autoantibodies in pregnant women and analyzed their association with fetal development.

## 2. Methods

### 2.1. Ethics and data protection

Written informed consent was received from all participants prior to

study inclusion. Analyses were approved by Charité ethics committee (EA2/220/20). Samples were handled with pseudonymized identifiers and investigators blinded to the status of donor and fetus.

### 2.2. Clinical data

Pregnant women presenting for antenatal care in the involved prenatal diagnostic centers between June 2021 and November 2021 were recruited, <10% refused to participate in the study. The vast majority of women underwent routine ultrasound check-ups without suspected pregnancy problems, no trial specific tests were performed. Medical information was acquired by questionnaire, interview, and from medical documentation. Blood was drawn during pregnancy, for a subcohort also at birth (maternal serum and umbilical cord blood). Controls consisting of non-pregnant healthy donors and clinically isolated syndrome (CIS)/relapsing-remitting multiple sclerosis (RRMS) patients were recruited via the DZNE Berlin and the neuroimmunology trial facility at the NeuroCure Clinical Research Center of Charité (NCT01371071, [clinicaltrials.gov](https://clinicaltrials.gov)), respectively. Statistical analysis was performed using Chi-square and Fisher's exact test, as appropriate.

### 2.3. Cell-based assay

Synapsin-Ib cell-based assay (CBA) was performed as previously described (Höltje et al., 2017). In brief, human embryonic kidney (HEK293T) cells transiently transfected with human synapsin-Ib were methanol-fixed, incubated overnight at 4 °C with sera diluted 1:300 and IgG binding detected with goat anti-human IgG AF488-antibody (Dianova, #109-545-003). For co-stainings, commercial rabbit synapsin-I/II antibody (Synaptic Systems, #106002) and anti-rabbit IgG AF594-antibody (Jackson IR, #111-585-003) were used. The CBA was scored using a semi-quantitative scale by two independent investigators: 0 indicated no binding, 1 unspecific signals ('background'), and 2 intensive binding ('positive') (Fig. 1A). To exclude non-specific HEK293T cell binding, all sera were tested on control cells overexpressing the NR1 subunit of the NMDA receptor (after methanol fixation) or CASPR2 (after paraformaldehyde fixation), and synapsin CBA-positive sera were also tested on untransfected HEK293T cells (fixed and handled identical to synapsin-transfected cells).

Titration of synapsin-Ib-positive sera were performed using serial dilutions (1:300, 1:1,000, 1:3,000, 1:10,000, 1:30,000, 1:100,000). IgG subclasses were detected using mouse anti-human-IgG1, -IgG2, -IgG3 and -IgG4 AF647-antibodies (SouthernBiotech #9052-31, #9070-31, #9210-31, #9200-31). Data analysis was performed by two independent raters (IB, HP) with identical results in >95% of cases (and less than ±1 titer steps in the remaining cases).

### 2.4. Primary neuronal cultures

Rat neuronal cultures were generated as previously described (Turko et al., 2019a, 2019b). In brief, neocortical tissue was extracted from wild type Wistar rat pups, dissociated in papain (1.5 mg/ml; Merck) for 30 min at 37 °C and triturated in bovine serum albumin (BSA; 10 mg/ml; Merck). Cells were counted and resuspended in Neurobasal A medium (supplemented with 1 × B27, 1 × GlutaMax, and 100 U/ml Penicillin-Streptomycin; ThermoFisher Scientific). Dissociated cells were grown on μ-Slide 8-well chambered coverslips (ibidi, #80807) previously coated for 1 h with poly-L-lysine hydrobromide (20 μg/ml, Merck). Cells were plated in 20 μl droplets at a density of 2000 cells/μl and cultured in humidified conditions at 37 °C and 5% CO<sub>2</sub> until harvesting at DIV 20–22 followed by fixation in 2% paraformaldehyde for 10 min. The neuronal cultures were incubated overnight with sera diluted 1:200 including 0.01% TritonX for permeabilization. Goat anti-human IgG AF488-antibody (Dianova, #109-545-003) was used to detect human IgG. Following commercial antibodies were used for co-stainings: chicken MAP2 polyclonal antibody (ThermoFisher,

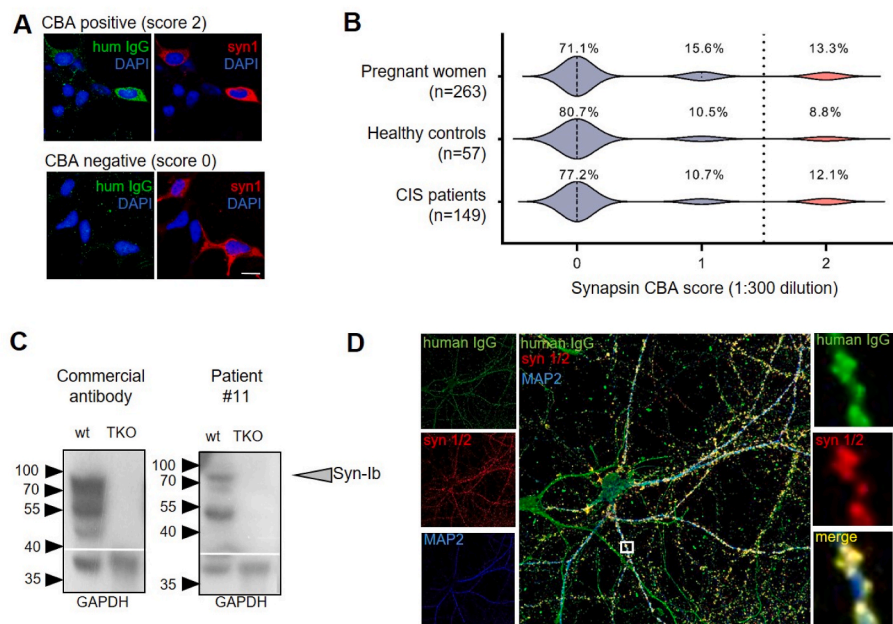


**Fig. 1.** High prevalence of synapsin-I autoantibodies in pregnant women. **(A)** Representative examples of immunofluorescence stainings with human sera at 1:300 dilution (green) with (top row) or without binding (bottom row) to HEK293 cells overexpressing human synapsin-Ib. Protein expression is confirmed with a commercial synapsin-I/II antibody (red). Nuclei are stained with DAPI (blue). Scale bar = 20  $\mu$ m. **(B)** Frequencies of synapsin-Ib autoantibodies in pregnant women and control cohorts, as determined by CBA. CBA scores: 0 = no binding, 1 = unspecific signal, 2 = intensive binding (positive); vertical dotted line represents cut-off for positivity. **(C)** Representative immunoblots of wild type (wt) and *Syn1/2/3* triple knock out (TKO) mice cortex homogenates with a commercial synapsin-I/II antibody as positive control and sera from CBA-positive pregnant women (1:200 dilution). The strong band at ~90 kDa corresponding to the molecular weight of synapsin-Ia/Ib was detected in wild type but not in TKO mouse tissue. Another band at ~50 kDa likely represents the synapsin-IIb isoform or breakdown products of synapsin-I. Detection of GAPDH served as loading control. **(D)** Immunofluorescence staining on rat hippocampal neurons demonstrated strong IgG binding of human sera (green) in a characteristic synaptic pattern (insert shows high magnification, MAP2 [blue] staining for better visualization of neuronal processes). The punctate staining

completely overlapped with a commercial synapsin antibody (red, insert for high magnification).

#PA1-16751), goat anti-chicken IgY (H + L) AF633 (ThermoFisher, #A-21103), rabbit anti-synapsin-I/II (Synaptic Systems, #106002), and anti-rabbit IgG AF594 (Jackson IR, #111-585-003).

## 2.5. Enzyme-linked immunosorbent assay (ELISA)

Recombinant rat EGFP-synapsin-I (Milovanovic et al., 2018) (200 ng) diluted in PBS were incubated overnight at 4 °C in 96-well high-binding plates. After blocking, sera diluted 1:200 in blocking solution (PBS containing 1% BSA, 0.05% Tween) were incubated for 1 h before adding an HRP-coupled anti-human IgG antibody (Dianova, #109-035-003) for 1 h and developed using Ultra TMB substrate solution. 450 nm absorbance values were corrected by subtraction of 630 nm absorbance and by a mean value of control wells containing no serum.

## 2.6. Western blotting

Cortices from wild type or *SYN1/2/3* triple knockout mice (TKO) were homogenized in RIPA buffer, and lysates were used for SDS-PAGE and Western blotting as described (Höltje et al., 2017). Membranes were incubated with CBA-positive sera (= CBA score 2) diluted 1:200. For Western blotting of transfected HEK293 cells, transfected cells were grown on 6-well plates and homogenized in phosphate-buffered saline (PBS) with protease inhibitors. Homogenates were used for SDS-PAGE and Western blotting. Untransfected cells served as control. A rabbit polyclonal synapsin-I/II antibody (Synaptic Systems, #106002) served as positive control to detect synapsin isoforms in brain lysates and transfected HEK cells. A monoclonal glyceraldehyde-3-phosphate dehydrogenase antibody (GAPDH, Merck Millipore, #MAB374) was used as loading control.

## 2.7. Automated $\mu$ SPOT synthesis

The complete human Synapsin-Ia and -Ib sequence was obtained from Uniprot (P17600, P17600-2) and displayed as 20-mer overlapping peptides shifted by 3 amino acid residues. In total, 231 Synapsin peptides were synthesized using MultiPep RSi robot (CEM, Kamp-Lintford,

Germany) on cellulose discs containing 9-fluorenylmethoxycarbonyl- $\beta$ -alanine linkers. Synthesis started by deprotecting the Fmoc-group using 20% piperidine in dimethylformamide (DMF). During the coupling step peptide chains were elongated using the following coupling solution consisting of amino acids (0.5 M) with oxyma (1 M) and diisopropylmethanediimine (1 M) in DMF (1:1:1). Coupling steps were followed by capping (4% acetic anhydride in DMF). Side chains were deprotected using the cleavage cocktail consisting of 90% trifluoroacetic acid (TFA), 2% dichloromethane (DCM), 5% H<sub>2</sub>O and 3% triisopropylsilane. Afterward, the cleavage cocktail was discarded, discs were dissolved overnight using a solvation mixture containing 88.5% TFA, 4% trifluoromethanesulfonic acid (TFMSA), 5% H<sub>2</sub>O and 2.5% triisopropyl silane (TIPS). Resulting peptide-cellulose conjugates (PCCs) were precipitated with ice-cold ether. The pellets were dissolved overnight in DMSO. PCCs solutions were diluted 2:1 with saline-sodium citrate buffer (150 mM NaCl, 15 mM trisodium citrate, pH 7.0) and transferred to white-coated CelluSpot blank slides (76  $\times$  26 mm, Intavis AG Peptide Services GmbH and CO. KG), using a SlideSpotter (CEM GmbH).

## 2.8. Epitope mapping

Synapsin slides were blocked for 60 min in 5% (w/v) skimmed milk powder 0.05% Tween20 PBS pH 7.4. Afterward, slides were incubated for 30 min with positive and negative serum as determined with cell-based assays (1:1000 dilution). Washing steps were carried out three times using 0.05% Tween20 PBS. IgG antibodies were detected using goat-anti-human secondary antibodies (Thermo Fisher, #31410, 1:2500). Chemiluminescence signal was detected with an Azure system c400 using SuperSignal West Femto maximum sensitive substrate (Thermo Scientific, Schwerte, Germany). Microarray binding intensities were quantified using the software-tool MARTin (<https://github.com/scitequest/martin>) and normalized to the most prominent binder. Heat-maps were generated with OriginPro 2021 9.8.0.200 (OriginLab, Northampton, MA). Human synapsin-I 3D model was extracted from AlphaFold (DeepMind Technologies, London, UK) (Jumper et al., 2021) database and rendered using Pymol 2.4 (Schrodinger Inc, New York, U.S.).

### 3. Results

Given the crucial role of synapsin-I in neurodevelopment, we aimed to screen for synapsin-I autoantibodies during pregnancy and to investigate their association with fetal development. We collected sera from 263 pregnant women ( $34 \pm 5$  years of age,  $25 \pm 8$  weeks of gestation; mean  $\pm$  SD) as well as clinical data (Table 1). Following an explorative approach and to reduce selection bias, there were no exclusion criteria for the recruitment of pregnant women.

First, all sera were screened for synapsin-Ib autoantibodies of IgG isotype using a previously established CBA (Höltje et al., 2017). In the visual scoring system for antibody binding, scores of 2 were considered CBA-positive (Fig. 1A) and detected in 35 (13.3%) pregnant women of our cohort (Fig. 1B) with antibody titers of up to 1:100,000 (Table 2). A similar prevalence was observed in control cohorts of healthy non-pregnant donors (8.8%, 5 of 75 subject) and CIS patients (12.1%, 18 of 147) (Fig. 1B). Eight of the 35 CBA-positive sera showed strong IgG binding to cortex homogenates of wild type mice at the expected molecular weight, which was completely abolished in *SYN1/2/3* TKO mice confirming antibody specificity to linear epitopes (Fig. 1C). Immunofluorescence staining on rat hippocampal neurons demonstrated strong IgG binding of human sera in a characteristic punctate synaptic pattern, completely overlapping with a commercial synapsin antibody (Fig. 1D).

We next analyzed clinical data related to the women's pregnancy courses and ultrasound findings of fetal development. While there were no differences in the pregnant women's age, gestational age, preexisting conditions, and medication between synapsin-I autoantibody-positive and -negative groups, we identified several defects to be significantly associated with the presence of synapsin-I autoantibodies (Table 1, Fig. 2A and B). In CBA-positive women fetal ultrasound revealed abnormal results more frequently than in CBA-negative women (OR: 3.1

[95% CI: 1.4–6.79],  $p = 0.004$ ). Likewise, fetal structural changes were more common in the CBA-positive group (OR 4.9 [1.96–12.35],  $p < 0.001$ ). Although developmental changes in the central nervous system were not different between both groups, the fetuses of the CBA-positive women displayed an increased frequency of intrauterine growth retardation (OR 6.5 [2.05–20.78],  $p = 0.003$ ) and amniotic fluid disorders (OR 4.1 [1.13–14.72],  $p = 0.044$ ). Moreover, we found that CBA-positive women more frequently had previous children with established neuropsychiatric disorders (OR 3.55 [1.33–9.46],  $p = 0.016$ ).

As expected from the physiological maternofetal transfer of IgG, synapsin autoantibodies were likewise detectable in the fetal circulation. Samples from umbilical cord blood showed similar autoantibody titers compared to maternal serum during birth, usually within one titer step (Fig. 2C). IgG1 and/or IgG3 were the predominant IgG subclasses in almost all women (Fig. 2D, Suppl. Fig. 1, Table 2). Given that IgG1 is the main subclass actively transported from maternal blood into the fetal circulation in humans, we next assessed the association of IgG1 and high-level autoantibodies (titers  $\geq 1:30,000$ ) with fetal abnormalities (Fig. 2E and F). Indeed, the combination of both was significantly more frequent in cases with intrauterine pathologies (Fig. 2F).

To further examine autoantibody binding epitopes, we analyzed all sera of the pregnant women in an in-house synapsin-I ELISA. Although the CBA-positive sera showed more intense mean binding to the immobilized recombinant synapsin-I, relatively weak correlation with broad overlap was detected between antibody levels in CBA and ELISA ( $r = 0.359$ ,  $p < 0.001$ , Fig. 3A). The most likely explanation is the prevailing autoantibody binding of some sera to conformational epitopes in the CBA, while epitopes measured in the ELISA may result from different folding during the purification procedure. Indeed, some sera with strong synapsin-I binding in the CBA lost signal in immunoblots of synapsin-I-overexpressing HEK293 cell homogenates, indicating that

**Table 1**  
Clinical data.

	Synapsin Ib CBA positive (n = 35)	Synapsin Ib CBA negative (n = 228)	P value <sup>l</sup>
Mother			
Age (years)	34 ( $\pm 5$ )	33 ( $\pm 4$ )	
Chronic diseases	10 (28.6%)	42 (18.4%)	0.160
Autoimmune diseases <sup>a</sup>	3 (8.6%)	23 (10.1%)	1.000
Neuropsychiatric diseases <sup>b</sup>	3 (8.6%)	10 (4.4%)	0.391
Current medication	11 (12.6%)	76 (33.3%)	0.824
Immunomodulatory drugs <sup>c</sup>	2 (5.7%)	6 (2.6%)	0.289
History of current pregnancy			
Gestational week	25 ( $\pm 8$ )	25 ( $\pm 8$ )	
Ultrasound abnormalities	12 (34.3%)	33 (14.5%)	<b>0.004</b>
Structural abnormalities <sup>d</sup>	8 (22.9%)	9 (3.9%)	<b>&lt; 0.001</b>
CNS abnormalities <sup>e</sup>	1 (2.9%)	6 (2.6%)	1.000
Growth retardation	6 (17.1%)	7 (3.1%)	<b>0.003</b>
Macrosomia	1 (2.9%)	5 (2.2%)	0.579
Amniotic fluid disorders <sup>g</sup>	4 (11.4%)	7 (3.1%)	<b>0.044</b>
Infections during pregnancy <sup>h</sup>	2 (5.7%)	5 (2.2%)	0.235
Pregnancy-related diseases <sup>i</sup>	7 (20.0%)	51 (22.4%)	0.753
Previous pregnancies			
Gravida	2	2	
Para	1	1	
Miscarriages	0	0	
Complications during previous pregnancy or labor	7 (20.0%)	32 (14.0%)	0.355
Children with neuropsychiatric disorders	7 (20.0%)	15 (6.6%)	<b>0.016</b>

<sup>a</sup> Autoimmune diseases: Hashimoto thyroiditis (n = 11), Graves' disease (n = 1), type I diabetes (n = 3), multiple sclerosis (n = 3), systemic lupus erythematosus (n = 2), and ulcerative colitis (n = 2), sarcoidosis (n = 1), alopecia areata (n = 1), psoriasis (n = 1), reactive arthritis (n = 1).

<sup>b</sup> Neuropsychiatric diseases: depression (n = 8), multiple sclerosis (n = 3), attention deficit hyperactivity disorder (n = 1), schizophrenia, bipolar disorder (n = 1).

<sup>c</sup> Immunomodulatory drugs: prednisolone (n = 3), azathioprine (n = 1), beta interferons (n = 1), mesalazine (n = 1), budesonide (n = 1), vedolizumab (n = 1).

<sup>d</sup> Structural abnormalities: pulmonary (n = 2), cardiovascular (n = 7), renal (n = 4) and placenta/umbilical cord changes (n = 4).

<sup>e</sup> CNS abnormalities: agenesis of the corpus callosum (n = 2), spina bifida (n = 2) and others (n = 3).

<sup>g</sup> Amniotic fluid disorders: polyhydramnion (n = 7), anhydramnion (n = 1) and oligohydramnion (n = 4).

<sup>h</sup> Infections during pregnancy: streptococcus B (n = 2), hepatitis B (n = 2), others (n = 3).

<sup>i</sup> Pregnancy-related diseases: hypothyroidism (n = 24), gestational diabetes (n = 18), vaginal bleeding (n = 7), pre labor rupture of membranes (n = 1), cardiovascular (n = 3), total surgical cervical occlusion (n = 2), hyperemesis gravidarum (n = 1), cholestasis (n = 2), some patients developed more than one complication. Data are expressed as mean (SD) or frequency (%).

<sup>l</sup> P value was calculated using the Chi-square test (expected frequencies  $\geq 5$ ) and the Fisher's exact test ( $< 5$ ), as appropriate.

**Table 2**  
Summary of experimental synapsin-Ib antibody findings.

Patient N°	Syn-Ib CBA screening	Western blot (Brain) <sup>a</sup>	ELISA <sup>b</sup>	IgG sub-classes	Titer during pregnancy CBA	Titer at birth (mother) CBA	Titer at birth (child, umbilical cord blood) CBA	Titer at late follow-up <sup>c</sup> (mother) CBA
1	+	-	0.51	IgG3	1:30,000	1:3000	1:10,000	NA
2	+	-	0.29	IgG1, IgG3	1:30,000	1:30,000	NA	NA
3	+	-	0.09	IgG2	1:3000	1:3000	1:3000	NA
4	+	+	0.19	IgG3	1:1000	1:3000	1:1000	NA
5	+	-	0.15	IgG1	1:10,000	NA	NA	NA
6	+	-	0.30	IgG3	1:3000	NA	NA	NA
7	+	-	0.01	IgG1	1:100,000	1:100,000	1:30,000	NA
8	+	-	0.01	inc.	1:3000	1:10,000	1:3000	NA
9	+	-	0.16	IgG1	1:10,000	NA	NA	NA
10	+	-	0.16	inc.	1:10,000	1:30,000	1:30,000	1:30,000
11	+	+	0.07	inc.	1:10,000	1:3000	1:10,000	NA
12	+	-	0.20	inc.	1:10,000	NA	NA	NA
13	+	+	0.12	IgG1	1:100,000	1:10,000	1:100,000	NA
14	+	-	0.10	inc.	1:10,000	NA	NA	NA
15	+	-	0.24	IgG1	1:100,000	NA	NA	NA
16	+	-	0.17	inc.	1:30,000	NA	NA	NA
17	+	-	0.08	IgG1, IgG3	1:100,000	1:3000	1:1000	NA
18	+	-	0.54	IgG3	1:30,000	NA	NA	NA
19	+	+	0.27	IgG3	1:10,000	NA	NA	NA
20	+	-	0.38	IgG4	1:10,000	NA	NA	NA
21	+	-	0.44	IgG3	1:3000	NA	NA	NA
22	+	-	0.05	IgG1	1:10,000	NA	NA	NA
23	+	-	0.14	IgG1	1:1000	NA	NA	1:30,000
24	+	-	0.06	IgG1	1:100,000	NA	NA	NA
25	+	-	0.32	IgG3	1:30,000	NA	NA	NA
26	+	+	0.32	IgG3	1:3000	NA	NA	NA
27	+	-	0.11	IgG1	1:10,000	NA	NA	NA
28	+	+	0.24	inc.	1:100,000	NA	NA	NA
29	+	+	0.20	inc.	1:30,000	NA	NA	NA
30	+	-	0.17	IgG1	1:10,000	NA	NA	NA
31	+	-	0.08	inc.	1:10,000	NA	NA	NA
32	+	-	0.04	IgG1, IgG3	1:10,000	NA	NA	1:30,000
33	+	-	0.04	inc.	1:30,000	NA	NA	NA
34	+	+	0.10	IgG2	1:10,000	1:10,000	1:30,000	NA
35	+	-	0.13	IgG1	1:10,000	1:10,000	1:30,000	NA

*Inc.*, samples were repeatedly tested but results remained inconclusive. *NA*, samples were not available.

<sup>a</sup> Western blots using mouse brain cortex homogenates, (+) indicates detection of binding in wild type and loss of binding in Syn1/2/3 triple knock out mice.

<sup>b</sup> ELISA for detection of autoantibody binding to recombinant synapsin-Ib (mean of 2 independent measurements), values are optical density (OD) at 450 nm.

<sup>c</sup> Sub-cohort with another serum samples >1 year after giving birth.

protein linearization with loss of conformational structures abolished reactivity (Fig. 3B).

Next, we fine-mapped IgG autoantibody binding sites using a synapsin-I peptide microarray approach (Fig. 3C) (Talucci and Maric, 2023; Schulte et al., 2023). Using overlapping 20-mer peptides shifted by three amino acid residues, we identified five target epitopes from four autoantibody-positive sera, while binding for these epitopes was absent in all tested CBA-negative sera. Four of these epitopes are located in intrinsically disordered regions within the domains A, B and D, while one synapsin-I epitope mapped to a structured region within domain C (Fig. 3D).

#### 4. Discussion

For this study, we recruited a clinical cohort of 263 pregnant women and provide data on the frequency of synapsin-I autoantibodies during pregnancy as well as associations with fetal development. Using a CBA, synapsin-I IgG autoantibodies had a seroprevalence of 13.3% during pregnancy. Most of tested sera were negative on Western blots under denaturing conditions, indicating a conformational dependency of their target binding, a phenomenon well known from other human autoantibodies including those against NMDA receptors (Gleichman et al., 2012). Epitope mapping identified five immunogenic regions on synapsin-Ib, three of which were localized at the D domain, a part of synapsin-I that had already been identified as main target domain in a previous study investigating patients with psychiatric and neurological disorders (Mertens et al., 2018). Domain D is necessary for synapsin-I

liquid-liquid phase separation (LLPS), a process in which biomolecules segregate from surrounding solution without any limiting membrane or a scaffold forming so-called biomolecular condensates (Milovanovic et al., 2018; Banani et al., 2017). Synaptic vesicles (SVs) cohorts form such condensates at the synaptic bouton through LLPS of synapsins (Sansevino et al., 2023). Injection of antibodies specifically directed towards domain D disrupted the SV condensates in synapses at rest (Pechstein et al., 2020). It is tempting to speculate that the human autoantibodies that we detected could directly impede the process of synapsin/SV condensation.

Blinded clinical analyses in the present study showed that synapsin-I autoantibodies were strongly associated with several abnormalities of fetal development including intrauterine growth retardation, indicating that the autoantibodies can be a clinically useful biomarker of abnormal fetal development or even directly participate in the disease process. Effects were particularly strong in cases with high synapsin autoantibody levels and IgG1 predominance, the subclass with strongest transmission into the fetal circulation during pregnancy. Examination of umbilical cord blood showed that synapsin autoantibodies reach the fetal blood to similar (and in some cases even higher) levels seen in the mothers.

Thereby, the frequency of synapsin autoantibodies in pregnancy clearly surpasses frequencies of IgG autoantibodies to other neuronal targets as reported in healthy donors (<2% for 9 tested antigens) (Dahm et al., 2014) and in mothers of children with neuropsychiatric deficits (4.1% for CASPR2) (Coutinho et al., 2017). Interestingly, autoantibody frequency was in the same range as in our two control cohorts,

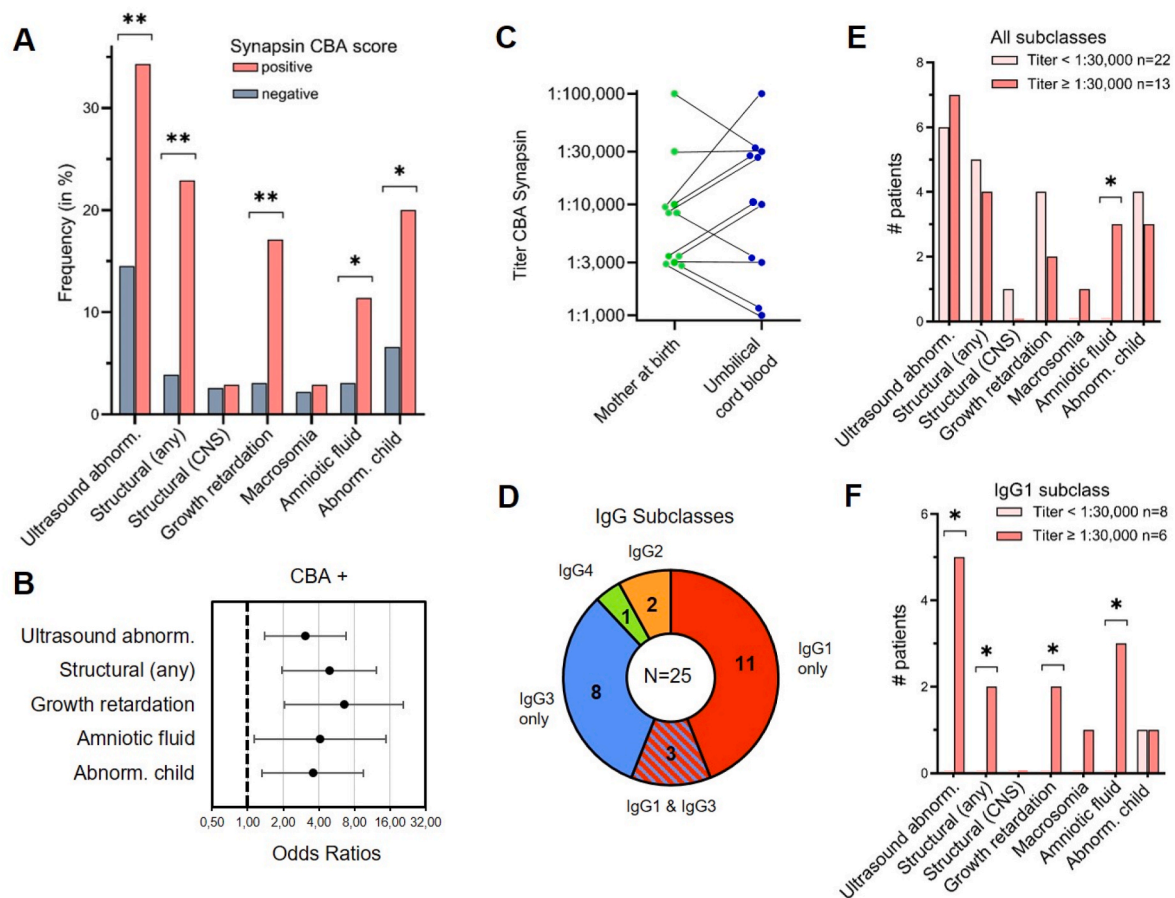


**Fig. 2.** Strong, titer-dependent association of synapsin-I autoantibodies with abnormalities of fetal development during pregnancy. (A–B) Several ultrasound parameters and status of having previous children with neuropsychiatric disorders were significantly associated with the presence of synapsin-I autoantibodies in serum of pregnant mothers (A), with odds ratios of 3–7 (B). Statistical analysis used Fisher’s exact test when expected frequencies were <5 or Chi-square test with expected frequencies  $\geq 5$ , \* representing  $p < 0.05$ , \*\* $p < 0.01$  and \*\*\* $p < 0.001$ . (C) Synapsin autoantibodies reached the fetal circulation and were present with similar titers ( $\pm 1$  titer step, in one case 2 titer steps) in umbilical cord blood. (D) Synapsin autoantibodies were of IgG1 and/or IgG3 subclass in almost all pregnant women. (E) While the autoantibody titer alone did not discriminate between pathological and normal findings during fetal development (left), the combination of IgG1 subclass with high-level titers ( $\geq 1:30,000$ ) was significantly associated with abnormal measurements (right).

stimulating the intriguing question of whether potential autoantibody effects are absent or compensated in healthy subjects, but become visible only under certain conditions such as maternofetal autoantibody transfer. Extensive clinical follow-ups will disclose whether children from seropositive mothers are at risk to develop a specific phenotype, and whether it can even be attributed to certain binding epitopes within synapsin-I. The study markedly expands earlier findings of synapsin-I autoantibodies in women having a child with established neurodevelopmental disorders (Büniger et al., 2023) by showing that the autoantibody-associated risk may already be assessed during pregnancy.

The present study has several limitations. First, related to the study design, we cannot provide definite data of synapsin autoantibody pathogenicity and for a causal role for the developmental abnormalities seen during pregnancy. It is likely that different mechanisms can contribute, related to variable epitopes, IgG subclasses, titers, and host factors involving fetus and mother. Second, potential effects within and outside the central nervous system in the children were not further examined after birth in this study. Third, clinical data were generated from patient charts, ultrasound documentation and questionnaires during routine assessment, but were not specifically designed for the study. This may have resulted in less systematically collected, partially incomplete clinical data. Thus, prospective follow-up studies should follow a strict trial design regarding clinical assessment, laboratory and ultrasound findings.

While previous experimental data showed that synapsin

autoantibodies can reach their intracellular neuronal target through endocytosis and cause pathogenic effects *in vitro* (Rocchi et al., 2019), their role on neurophysiological function and neurodevelopment after transplacental exposure is unclear. Experimental maternofetal transfer models using antineuronal autoantibodies to other targets (Jurek et al., 2019; Brimberg et al., 2016; Mader et al., 2022) have recently substantiated a broader disease principle of neuropsychiatric morbidity resulting from autoantibody exposure during pregnancy. Similar studies are needed for synapsin autoantibodies and should preferentially be performed with patient-derived monoclonal antibodies to exclude possible interference with other serum antibodies. These experiments will help to elucidate whether transplacental synapsin autoantibodies can be directly pathogenic *in vivo*, which seems plausible given that synapsins constitute  $\sim 9\%$  of the total synaptic vesicle proteins (Khvotchev et al., 2009) and play a key role in brain development and synaptogenesis. In this case, the here identified distinct autoantibody epitopes within synapsin-I may provide starting points for antibody-neutralizing prophylactic strategies with the potential to prevent lifelong neuropsychiatric morbidity in affected children. Although further experimental work, prospective expansion of cohorts of healthy subjects and pregnant women, and refined epidemiological studies are needed, the present data already delineate how detection of maternal synapsin autoantibodies could change clinical routine algorithms during or even before pregnancy in the future.

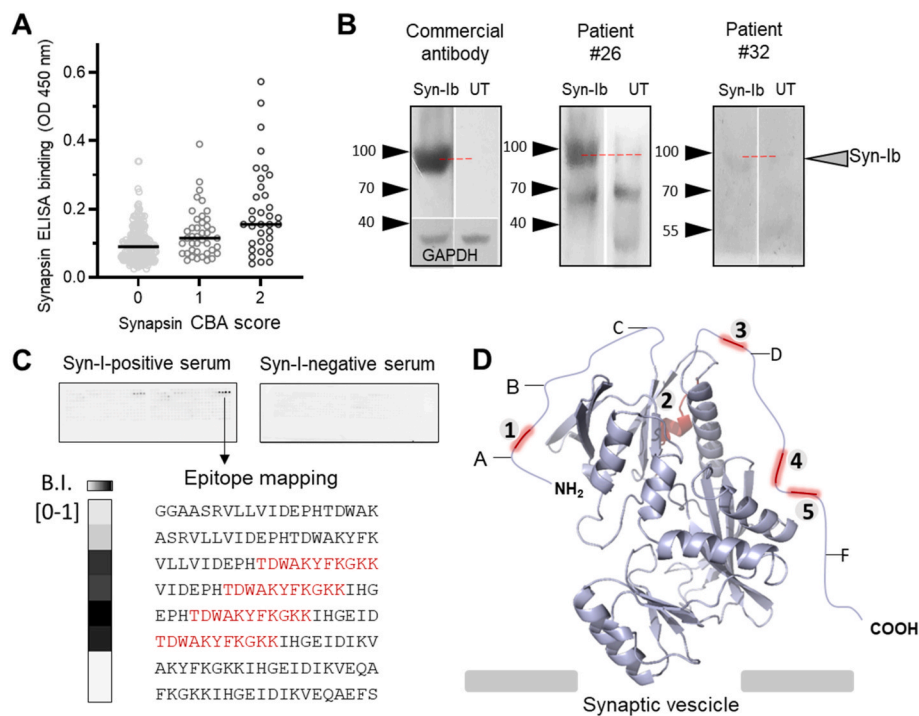


**Fig. 3.** Detection of synapsin-I autoantibodies by ELISA, immunoblotting and microarray-based epitope mapping. **(A)** ELISA-based screening of all human sera using recombinant synapsin-I correlated with autoantibody binding in the CBA. **(B)** Immunoblots of synapsin-Ib-transfected HEK293 cells confirm that some human sera (1:200 dilution) strongly detect the synapsin-Ib band (middle), while in others binding to non-conformational epitopes is lost (right). Commercial synapsin-I/II antibody served as positive control (left, GAPDH is exemplarily shown; UT = untransfected cells). **(C)** An overlapping peptide library containing 20-mer peptides with an off-set of three amino acids was designed to fully cover synapsin-I primary sequence. Microarrays were probed with autoantibody-positive and -negative serum. The representative example shows detection of IgG epitope 2 within the synapsin-I slides and a representative negative control serum. Heat map visualization: IgG binding intensities are displayed in grayscale (0 = no binding, 1 = maximal binding). The core shared motif is highlighted in red. **(D)** Synapsin-I domain architecture together with a cartoon representation of the alpha-fold model of synapsin-I visualized in Pymol. Mapped synapsin-I autoantibody epitopes (1–5, marked in red) are located in domain A-B (epitope 1, peptide sequence: <sup>28</sup>PQPPPPPPGAH<sup>38</sup>), domain C (epitope 2, <sup>124</sup>TDWAKYFKGKK<sup>134</sup>) and domain D (epitope 3: <sup>472</sup>PGPQRQGPPLQ<sup>482</sup>; 4: <sup>583</sup>GGQQRQGPQK<sup>592</sup>; 5: <sup>610</sup>VPRTPPTTQQPR<sup>623</sup>).

## Funding

This work was supported by grants from the German Research Foundation (DFG) (grants FOR3004, PR1274/4-1, PR1274/5-1, PR1274/9-1), the Helmholtz Association (HIL-A03), the German Federal Ministry of Education and Research (Connect-Generat 01GM1908D), the Einstein Stiftung Fellowship through the Günter Endres Fond, and the Sonnenfeld-Stiftung. J.K. is participant in the Berlin Institute of Health (BIH)-Charité Clinician Scientist Program. D.M. is supported by start-up funds from DZNE and the German Research Foundation (SFB MI 2104 and 1286/B10). I.T., K.O.K. and H.M.M. are supported by the Interdisziplinäres Zentrum für Klinische Forschung (IZKF) of Würzburg (A-F-N-419), German Research Foundation (MA6957/1-1), and the GSLS-Fellowship of the Graduate School of Life Sciences of the University of Würzburg.

## Author contributions

Conceptualization: A.M.K. and H.P.; Patient recruitment (pregnant women and healthy controls): I.B., K.L.M., T.U., E.S., J.M., S.V., W.H. and R.C.; Patient recruitment (CIS patients): F.P.; CBA, cell cultures and ELISA testing: I.B., J.K., H.F.R., S. v.H., M.H., C.H. C.C.-G., P.T. and D. M.; Western blotting M.H.; Microarray synthesis, assay and analysis: K. O.K., I. T. and H.M.M. Data analysis and visualization: I.B. and J.K.; Resources: A.M.K. and H.P.; Writing – original draft: I.B., J.K. and H.P.; Writing – review & editing: all authors.

## Declaration of generative AI and AI-assisted technologies in the writing process

During the preparation of this work the authors used no generative AI and AI-assisted technologies.

## Declaration of competing interest

The authors declare that they have no known competing financial interests or personal relationships that could have appeared to influence the work reported in this paper.

## Data availability

Data will be made available on request.

## Acknowledgements

We thank Stefanie Bandura, Matthias Sillmann, Doreen Brandl, Jennifer Bergander, Sonja Blumenau, Antje Dräger, Monika Majer and Petra Loge for excellent technical assistance and study nurse support. Synapsin triple KO mice were a generous gift from Fabio Benfenati (Istituto Italiano di Tecnologia, Genova).

## Appendix A. Supplementary data

Supplementary data to this article can be found online at <https://doi.org/10.1016/j.bbih.2023.100678>.

## References

- Banani, S.F., Lee, H.O., Hyman, A.A., Rosen, M.K., 2017. Biomolecular condensates: organizers of cellular biochemistry. *Nat. Rev. Mol. Cell Biol.* 18 (5), 285–298.
- Braniste, V., Al-Asmakh, M., Kowal, C., et al., 2014. The gut microbiota influences blood-brain barrier permeability in mice. *Sci. Transl. Med.* 6 (263), 263ra158.
- Brimberg, L., Mader, S., Jeganathan, V., et al., 2016. Caspr2-reactive antibody cloned from a mother of an ASD child mediates an ASD-like phenotype in mice. *Mol. Psychiatr.* 21 (12), 1663–1671.
- Bünger, I., Makridis, K.L., Kreye, J., et al., 2023. Maternal synapsin autoantibodies are associated with neurodevelopmental delay. *Front. Immunol.* 14, 1101087.
- Coutinho, E., Jacobson, L., Pedersen, M.G., et al., 2017. CASPR2 autoantibodies are raised during pregnancy in mothers of children with mental retardation and disorders of psychological development but not autism. *J. Neurol. Neurosurg. Psychiatry* 88 (9), 718–721.

- Coutinho, E., Jacobson, L., Shock, A., Smith, B., Vernon, A., Vincent, A., 2021. Inhibition of maternal-to-fetal transfer of IgG antibodies by FcRn blockade in a mouse model of arthrogryposis multiplex congenita. *Neurol Neuroimmunol Neuroinflamm* 8 (4).
- Dahm, L., Ott, C., Steiner, J., et al., 2014. Seroprevalence of autoantibodies against brain antigens in health and disease. *Ann. Neurol.* 76 (1), 82–94.
- De Camilli, P., Benfenati, F., Valtorta, F., Greengard, P., 1990. The synapsins. *Annu. Rev. Cell Biol.* 6, 433–460.
- Fornasiero, E.F., Bonanomi, D., Benfenati, F., Valtorta, F., 2010. The role of synapsins in neuronal development. *Cell. Mol. Life Sci.* 67 (9), 1383–1396.
- García, C.C., Blair, H.J., Seager, M., et al., 2004. Identification of a mutation in synapsin I, a synaptic vesicle protein, in a family with epilepsy. *J. Med. Genet.* 41 (3), 183–186.
- Gleichman, A.J., Spruce, L.A., Dalmau, J., Seeholzer, S.H., Lynch, D.R., 2012. Anti-NMDA receptor encephalitis antibody binding is dependent on amino acid identity of a small region within the GluN1 amino terminal domain. *J. Neurosci.* 32 (32), 11082–11094.
- Höltje, M., Mertens, R., Schou, M.B., et al., 2017. Synapsin-antibodies in psychiatric and neurological disorders: prevalence and clinical findings. *Brain Behav. Immun.* 66, 125–134.
- Jumper, J., Evans, R., Pritzel, A., et al., 2021. Highly accurate protein structure prediction with AlphaFold. *Nature* 596 (7873), 583–589.
- Jurek, B., Chayka, M., Kreye, J., et al., 2019. Human gestational N-methyl-d-aspartate receptor autoantibodies impair neonatal murine brain function. *Ann. Neurol.* 86 (5), 656–670.
- Khvotchev, M.V., Sun, J., 2009. Synapsins. In: Squire, L.R. (Ed.), *Encyclopedia of Neuroscience*. Academic Press, Oxford, pp. 705–708.
- Kreissner, K.O., Faller, B., <https://github.com/scitequest/martin>.
- Mader, S., Brimberg, L., Vo, A., et al., 2022. In utero exposure to maternal anti-aquaporin-4 antibodies alters brain vasculature and neural dynamics in male mouse offspring. *Sci. Transl. Med.* 14 (641), eabe9726.
- Mertens, R., Melchert, S., Gitler, D., et al., 2018. Epitope specificity of anti-synapsin autoantibodies: differential targeting of synapsin I domains. *PLoS One* 13 (12), e0208636.
- Milovanovic, D., Wu, Y., Bian, X., De Camilli, P., 2018. A liquid phase of synapsin and lipid vesicles. *Science* 361 (6402), 604–607.
- Pechstein, A., Tomilin, N., Fredrich, K., et al., 2020. Vesicle clustering in a living synapse depends on a synapsin region that mediates phase separation. *Cell Rep.* 30 (8), 2594, 602.e3.
- Prüss, H., 2021. Autoantibodies in neurological disease. *Nat. Rev. Immunol.* 21 (12), 798–813.
- Rocchi, A., Sacchetti, S., De Fusco, A., et al., 2019. Autoantibodies to synapsin I sequester synapsin I and alter synaptic function. *Cell Death Dis.* 10 (11), 864.
- Rosahl, T.W., Spillane, D., Missler, M., et al., 1995. Essential functions of synapsins I and II in synaptic vesicle regulation. *Nature* 375 (6531), 488–493.
- Sansevrino, R., Hoffmann, C., Milovanovic, D., 2023. Condensate biology of synaptic vesicle clusters. *Trends Neurosci.*
- Schulte, C., Khayenko, V., Maric, H.M., 2023. Peptide microarray-based protein interaction studies across affinity ranges: enzyme stalling, cross-linking, depletion, and neutralization. *Methods Mol. Biol.* 2578, 143–159.
- Südhof, T.C., Czernik, A.J., Kao, H.T., et al., 1989. Synapsins: mosaics of shared and individual domains in a family of synaptic vesicle phosphoproteins. *Science* 245 (4925), 1474–1480.
- Talucci, I., Maric, H.M., 2023. Peptide microarrays for studying autoantibodies in neurological disease. *Methods Mol. Biol.* 2578, 17–25.
- Turko, P., Groberman, K., Kaiser, T., Yanagawa, Y., Vida, I., 2019a. Primary cell culture of purified GABAergic or glutamatergic neurons established through fluorescence-activated cell sorting. *J. Vis. Exp.* (148).
- Turko, P., Groberman, K., Browa, F., Cobb, S., Vida, I., 2019b. Differential dependence of GABAergic and glutamatergic neurons on glia for the establishment of synaptic transmission. *Cerebr. Cortex* 29 (3), 1230–1243.
- Zhang, M., Augustine, G.J., 2021. Synapsins and the synaptic vesicle reserve pool: floats or anchors? *Cells* 10 (3).